Hindawi Publishing Corporation
Indian Journal of Materials Science
Volume 2014, Article ID 897125, 10 pages
http://dx.doi.org/10.1155/2014/897125

Review Article

Searching for Alternative Plasmonic Materials for Specific Applications

Amit Bansal and S. S. Verma

Department of Physics, SLIET, Longowal, Sangrur District, Punjab 148106, India

Correspondence should be addressed to S. S. Verma; ssverma@fastmail.fm

Received 22 February 2014; Revised 3 April 2014; Accepted 8 April 2014; Published 12 May 2014

Academic Editor: Subrata Kundu

The localized surface plasmon resonance (LSPR) based optical properties such as light scattering, absorption, and extinction efficiencies of multimetallic and metal-semiconductor nanostructures will be studied. The effect of size, surrounding medium, interaction between the particles, composition of the particles, and substrate on LSPR peak position, its line width, and maxima of cross-sections will also be discussed to optimize the selected systems for various applications like plasmonic sensors and biomedical applications and to enhance the efficiency of solar cells. Therefore, by varying all these factors, the LSPR peak of multimetallic and metal-semiconductor nanostructures can be tuned over the entire UV-visible to infrared (IR) region of the electromagnetic spectrum. Moreover the optical properties of underlying semiconductor materials can be enhanced by combining the semiconductor with noble metal nanoparticles.

1. Introduction

Plasmonics, which is the property of metal nanostructures due to surface plasmons, has become one of the most expanding fields in nanoscience. The goal of plasmonics is to control, tune, and manipulate light on the nanometer scale using the properties of collective electron excitations, known as surface plasmons. In plasmonic nanoparticles, the localized surface plasmon resonance (LSPR) supported at the optical frequencies where resonance occurs due to the collective excitation of conduction electrons, in response to the electric field component of the irradiated electromagnetic (EM) waves [1]. This is due to the fact that while oscillating EM wave incident on the conduction electrons of the metal nanoparticles, which are confined to the small volume, the conduction band electrons starts oscillate collectively with respect to the positive framework that leads to the charge separation at the nanoparticle surface and results in the production of restoring force [2] as shown in Figure 1.

The main need for LSPR is a large negative real part and a small imaginary part of the dielectric constant of the material. There are a large number of metals, that is, Li, Na, Al, Pb, Cd, In, and Ga, which satisfies this criterion and their plasmon resonances lie in the UV-Vis to infrared (IR) region of the EM spectrum. Most of these metals are rapidly oxidized and become unstable, and hence it is difficult to work with them [3], but the metals such as Au, Ag, and Cu attracted much attention because they are nobler in nature and able to form stable colloids with surrounding environment. Moreover, for these metals the LSPR peak lies in the visible region of the EM spectrum [4–6]. Here, the metals Ag and Cu are also unstable due to their rapid oxidation with the surrounding environment but recent development in synthesis techniques and new synthesis methods are able to synthesize these metals in stable form [3, 7].

The property of LSPR causes the large extinction cross-section in comparison to the geometrical cross-section of the nanoparticle. This is due to the strong EM field enhancement that occurs in the vicinity of the metal nanoparticle. Hence, because of this, the noble metal nanoparticles can be used in a variety of emerging applications like biomedical applications if the LSPR of noble metals lies in infrared region (IR) of the EM spectrum [8], large EM field enhancement around the surface of metal nanoparticles is used for surface enhanced Raman spectroscopy (SERS) [9], surrounding medium refractive index sensitivity of LSPR makes the use

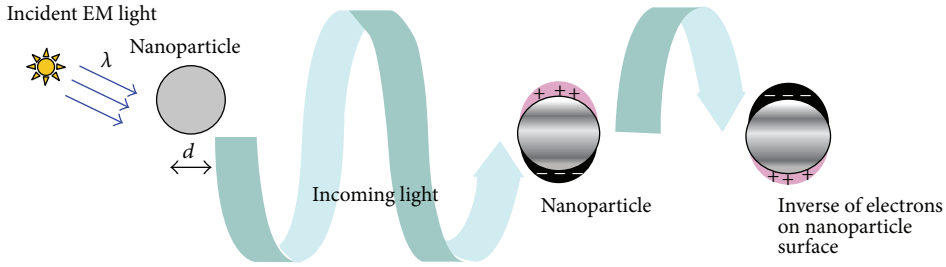

Figure 1: Schematics for plasmon oscillations.

of metal nanoparticles for plasmonic sensing [10, 11], large scattering from metal nanoparticles can be used to increase the efficiency of thin-film solar cells [12, 13], and so forth. The LSPR of noble metal nanoparticles can be tuned from UV-visible to IR region of the EM spectrum by controlling the factors such as size, shape, surrounding medium refractive index [2, 14, 15], and the composition of metal nanoparticle [16–18].

The optical properties of the gold colloidal solutions were firstly studied by Faraday but he was unable to identify the morphology of the gold nanoparticles and also unable to measure the size due to lack of methods available. Later, in 1908, Mie explained the origin of red color of gold colloids and he successfully studied the effect of the size and nonabsorbing surrounding medium on the optical properties of a single spherical nanoparticle by providing the exact solution of Maxwell's equations [19]. Gans extended the Mie theory for the optical properties of spheroidal such as oblate and prolate shaped nanoparticles [20]. Aden and Kerker in 1951 were the first who extended the Mie theory for coated nanospheres [21] and, then, many researches have given the algorithms to study the optical properties of coated multilayer spheres [22–25] but the code given by Bohren and Huffman is mostly used to describe the scattering properties of a coated sphere [26]. Recently, a computer code has been developed by Rodriguez et al. [27] on the basis of Yang's algorithm [25] which performs the calculations of optical properties of multilayered sphere.

The optical properties of individual noble metal nanoparticles of different shapes and sizes in different surrounding medium for different applications have been studied by many researchers [2, 3, 6, 10, 14–16, 28, 29]. Among the noble metal nanoparticles, Au and Ag have attracted much attention due to their excellent optical properties in the visible regime of EM spectrum [30–32]. Recently, Sureka and Santhanam investigate the optical properties of nanoparticles having different sizes, shapes, and composition by discrete dipole approximation (DDA) method for sensing and biomedical applications [33]. Hao and Nordlander studied the optical properties of Ag and Au nanoparticles by using FDTD simulations and show that the calculated spectra agree well with the exact calculations done by using experimentally measured dielectric functions [34]. Au is more costly than Ag and Cu, and Ag has high scattering efficiency [12] but is not stable under embedding conditions. Studies reported on Cu nanoparticles have also less favorable optical properties because of their oxidation in air or embedding conditions [35, 36]. Therefore, for cost-effective practical applications, the LSPR based optical properties can be enhanced and tuned in large region of the EM spectrum by combining the individual metals. Moreover, the advancement in synthesis of bimetallic (alloys or core-shell) nanostructures [37–40] with their unique optical, catalytic, electric, and magnetic properties in comparison with the individual metal particles makes them prospective candidates for cost-effective practical applications [41–43].

Shah et al. [44] provides the complete detailed synthesis of bimetallic nanoparticles and, recently, Tan and Cheong [36] summarized the synthesis of Ag-Cu alloy nanoparticles of wide size range and various shapes via chemical reduction route by utilizing different reagents such as metal initial precursors, stabilizers/surfactants, and reducing agents. The synthesis of individual metal and alloy nanoparticles is relatively simple, low in cost, less time consuming, and easy to control the particle size by chemical reduction method. The bimetallic nanoparticles of Ag and Cu have also been synthesized by other methods like chemical coreduction method [45], microwave assisted chemical reduction method in aqueous medium [46], polyol process [47], low temperature formation using hydrogen bombardment of thin films deposited on glass substrate [48], vapor phase codeposition method [42], and so forth. The other bimetallic nanoparticles of Ag and Au [49, 50], Au and Cu [17] have also been synthesized.

The optical properties of these multimetallic nanostructures can be tuned across the large region of the EM spectrum by controlling the core size, shell thickness, surrounding medium, and metal type in case of core-shell nanoparticles whereas, in case of alloy nanoparticles, in addition to size and surrounding medium, the composition of individual element also plays an important role. The LSPR peak position of the metal alloy nanoparticles lies in between the peak positions of two pure metals. Moreover a linear relationship between the LSPR peak position of the alloy nanoparticles and that of metal composition has been found by several researchers [17, 42, 46, 47]. In core-shell nanostructures, if thickness of shell layer is thin, then the EM field can interact with the core metal and leads to the excitation of corresponding LSPR so

that two distinct LSPR peaks corresponding to core and shell metal nanoparticles are observed. Whereas for thicker shell layer, the only LSPR due to shell layer is observed [50, 51].

The optical properties of individual noble metal and semiconductor nanostructures have been studied extensively in the literature [2, 28, 29, 52, 53] but their combined effect in optical properties has not been much explored. The combined synthesis of metal-semiconductor nanostructures leads to the new optical properties which are different from their individual materials [54–56] and paves the way for theoretical study. These new optical properties include the enhancement of the photocatalytic activities, optical absorption, photoluminescence, and nonlinear optical response of the given semiconductor material [55, 56] and shift in the LSPR of metal nanoparticles [54]. The excitation of LSPR in noble metal nanoparticle is due to the large EM field enhancement near the surface of metal nanoparticle and, when it is placed onto a semiconductor nanostructure, enhancement in optical absorption and photoluminescence of the semiconductor nanoparticle is seen [56–58]. Many reports have been proposed for enhancing the optical properties of semiconductors due to this phenomenon. Schaadt et al. [59] reported the enhancement in optical absorption of Si photodiodes across the large spectral region by depositing Au nanoparticles on its surface. Pradhan et al. [56] prepared the CdSe semiconductor film whose surface is coated with gold nanoparticles of different size and shows the enhancement in Raman intensity and photoluminescence of CdSe film. Repan and Pikker [60] investigate the light absorption inside the CdTe absorber layer doped by Ag, Au, Cu, and Al metal nanospheres and found the absorption enhancement up to 2.5 times with Ag or Au nanoparticles with diameters of 45–50 nm in the spectral range of 650–900 nm. Shaviv et al. [61] studied the absorption properties of metal-semiconductor hybrid nanoparticles by comparing experimental results with DDA simulations

The optical properties of underlying semiconductor materials can be enhanced by combining the semiconductor with that of noble metal nanoparticles. In the first case, when light is incident on semiconductor coated with noble metal nanoparticles, the incoming photons interact with the conduction electrons of metal and lead to the excitation of surface plasmons. The energy associated with these surface plasmons can be efficiently collected by the metal nanoparticles and transferred to the underlying semiconductor, hence enhancing the optical properties of semiconductor [56]. In the second case, when light is incident on noble metal coated with semiconductor nanoparticles, redshift in the LSPR peak of noble metal nanoparticle is observed. This is due to the coating of noble metal nanoparticle with the semiconductor material having high refractive index [54] and interaction between the semiconductor shell excitons and surface plasmons of noble metal core nanoparticles. This interaction is called excitons-plasmon interactions. Since both the metal and semiconductor nanomaterials exhibit excitations at their own optical frequencies, the excitations in semiconductor materials are defined by the transitions between discrete electronic levels, that is, conduction and valence bands, that lead to the formation of bound electron-hole pairs called excitons. Similarly in metal nanoparticles, the collective oscillation of conduction band electrons leads to surface plasmons resonances. The interactions between these excitons in semiconductors and surface plasmons in metal nanoparticles occur because dimensions of both are in nanoscale and also in close proximity [62]. In general, these metal-semiconductor nanostructures can be used in potential applications like optical sensing and light emitters and also increase the absorption efficiency and photoluminescence of semiconductors and so forth [55, 62]. Recently, Easawi et al. [63] show the enhancement in absorption of semiconductor shell at the cost of suppression of LSPR of core noble metal nanoparticle as the thickness of semiconductor shell is increased. This is due to the increase in the coupling strength of metal core plasmons and semiconductor shell excitons which leads to the transfer of charge and changes the electron density of metal nanoparticle.

Therefore, the present study theoretically describes the optical properties of noble multimetallic nanoparticles and semiconductors coated with metals for their potential use in future plasmonic applications and to enhance the optical characteristics of underlying semiconductor material. The effect of size, shape, surrounding medium, interaction between the particles, and their relative composition on the LSPR peak position has been studied. The retardation effects such as radiation damping, dynamic depolarization, and surface scattering have also been included.

2. Dielectric Properties of the Material

The behavior of surface plasmons of noble metal nanostructures can be made understandable on the basis of frequency dependent complex dielectric function, that is, $\varepsilon(\omega)$. The main contribution to the dielectric function is from the free conduction electrons (intraband transitions) in the bulk material and the interband transitions of bound electrons at high energy, usually in ultraviolet (UV) region. Therefore the dielectric constant can be given as

$$\varepsilon(\omega) = \varepsilon_{\text{int}ra}(\omega) + \varepsilon_{\text{int}er}(\omega). \quad (1)$$

Here, the interband contribution is due to the electronic transitions of the bound electrons from filled to the empty bulk band of the material and intraband contributions are given by Drude free electron model. In this model, Drude assumes a gas of independent electrons that can move freely and motion of whole free electrons is the sum of the motion of individual electrons. According to Drude [26],

$$\varepsilon_{\text{int}ra}(\omega) = 1 - \frac{\omega_p^2}{(\omega^2 + i\gamma\omega)}, \quad (2)$$

where ω is the optical frequency and γ is the bulk damping constant due to the scattering of free electrons from other electrons, phonons, impurities, and defects and ω_p is the bulk plasma frequency which is given as $\omega_p = \sqrt{4\pi n e^2/m_e^*}$, where n is the free electron density and e and m_e^* are the electronic charge and its effective mass. Therefore, the bulk plasma frequency depends only on the density of free

Table 1: Electron density and plasma frequency values of Au, Ag and Cu noble nanoparticles.

Noble metal	Electron density (10^{22}/cm^3)	Plasma frequency (10^{16} Hz)
Gold (Au)	5.90	1.40
Silver (Ag)	5.86	1.39
Copper (Cu)	8.47	1.64

electrons of the material. This plasma frequency for metals mainly lies in the UV-visible region with energies from 3 to 20 eV [14]. The electronic density of noble metals and their corresponding plasma frequencies are given in Table 1 (http://hyperphysics.phy-astr.gsu.edu/hbase/hframe.html).

Therefore dielectric function of the metal becomes

$$\varepsilon(\omega) = 1 - \frac{\omega_p^2}{\left(\omega^2 + i\gamma\omega\right)} + \varepsilon_{\text{int}\,er}(\omega). \tag{3}$$

The effects of intraband transitions are dominant at low energy region, that is, in the visible region, whereas the interband transitions are important at high energies, that is, in the UV region of the EM spectrum.

When dimension of the metal nanoparticle is comparable to or smaller than the electron mean free path which is of the order of few nanometers, then the electrons that experienced extra scattering form the boundary of the nanoparticle and dielectric constant of the material becomes size dependent.

This extra contribution due to small dimension of the metal nanoparticle is called electron surface scattering. The extra damping term, that is, $\gamma_{\text{sur}} = Av_f/a$, is to be added to the bulk damping constant in the expression of dielectric constant to include the effect of surface scattering. Where a is the dimension of the nanoparticle (width in case of nanorod, radius in case of sphere, and thickness in case of core-shell), v_f is the Fermi velocity of the electron and A is constant [26]. The effect of surface scattering is such that it broadens the resonant peak and reduces its intensity but does not change the peak position so far [14].

2.1. Retardation Effects. The retardation effects come into picture when dimensions of the metal nanoparticle are such that the oscillations of the conduction band electrons no longer remain homogenous. The effects such as radiation damping and dynamic depolarization contribute to the plasmonic peak with the generation of multipolar excitations at longer wavelengths, shift in the peak position, and decrease the intensity. Radiation damping arises due to the spontaneous emission of the radiation by the induced dipole and dynamic depolarization arises due to the nonhomogeneity response of the conduction electrons to the incident EM field; that is, oscillations of the free electrons no longer remain in phase. These effects grow rapidly with particle size and broadening of line width takes place. The effect of both terms can be included by using the following expression:

$$\frac{1}{\alpha} = \frac{1}{\alpha} - \frac{2}{3}ik^3 - \frac{k^2}{a}, \tag{4}$$

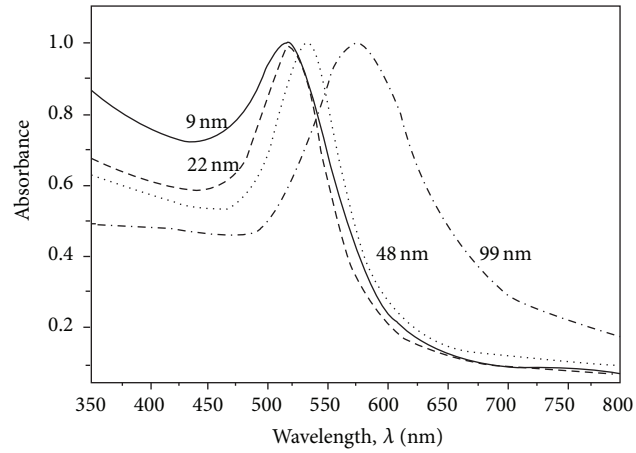

Figure 2: Absorbance spectra of Au nanospheres of different size. Reprinted from Link and El-Sayed [65].

where α and a are the polarizability and dimension of the nanoparticle, respectively. The first term represents the radiation damping contribution and the second term represents the dynamic depolarization contribution [2, 64].

3. Different Factors That Affect LSPR

The terms associated with the LSPR peak generated by noble metal nanoparticles, that is, LSPR peak position, its line width, and maxima of cross-sections, have been affected by nanoparticle size, shape, surrounding medium, interaction between the particles, composition of the particles, and substrate effect. Therefore, by varying all these factors, the LSPR peak of noble metal nanostructures can be tuned over the entire UV-visible to IR spectral region. The brief description of each factor is explained below.

3.1. Size Effect. The LSPR frequency of noble metal nanostructures is a strong function of the particle size. In the quasistatic approximation, the LSPR peaks are due to the excitation of the dipolar plasmon resonance mode whereas, with increase in the size, the LSPR peak shows redshift in the wavelength due to the decrease in resonant frequency as the restoring force decreases [65] (Figure 2) and higher order multipolar resonance modes also such as quadrupolar and octupolar exhibits. A relationship of these modes with real and imaginary dielectric constant of particle is given by [66]

$$\varepsilon_1 = -\left\{\frac{l+1}{l}\right\}\varepsilon_s, \tag{5}$$

where l represents the order of resonance mode and its value is 1 for dipolar mode, 2 for quadrupolar mode, 3 for octupolar mode, and so on.

These higher order modes exist due to the unsymmetrical charge distribution on the surface of metal nanoparticle and shift to the longer wavelength region as the particle size increases which further causes the broadening of LSPR peaks. The retardation effects such as dynamic depolarization

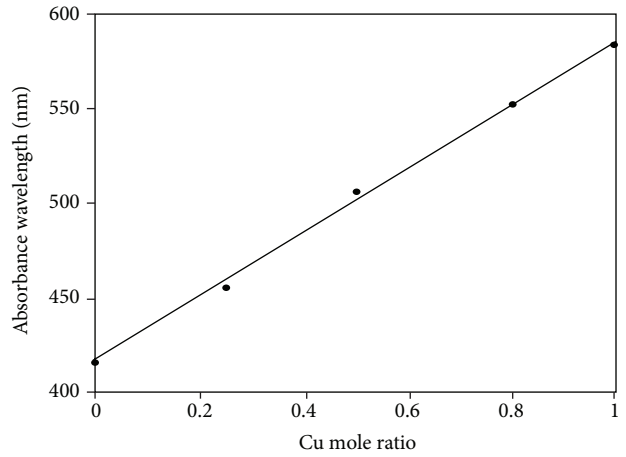

Figure 3: Plasmon absorption maximum of Ag-Cu alloy nanoparticles against the Cu mole ratio. Reprinted from Valodkar et al. [46].

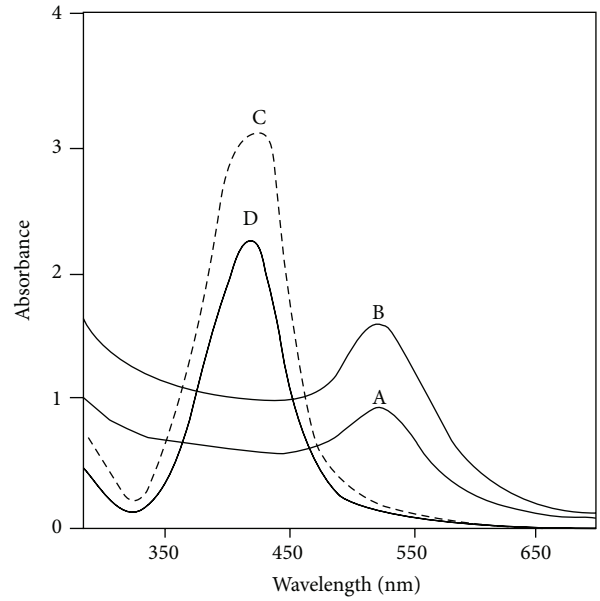

Figure 4: Absorption spectra of solutions of Au (A and B) and Ag (C and D) nanoparticles, measured using water (A and C) and hexane (B and D) as solvents. Reprinted from Hutter et al. [67].

and radiation damping affect the LSPR peak at such larger size, which contributes to the redshift of the LSPR in the wavelength region and peak broadening, respectively [65]. Moreover, with increase in particle size, the extinction spectra have more contribution from the scattering properties in comparison to the absorption properties [26].

3.2. Composition of the Nanoparticle. The optical properties of metallic nanoparticles can also be tuned by varying the composition of metallic nanoparticles. Recently alloys and core-shell nanoparticles have been given a lot of attention [15, 17, 18]. The alloy nanoparticle seems to be easy to handle because, generally, a linear relationship of the extinction maxima with that of metal composition is found both theoretically and experimentally as shown in Figure 3 [17, 46, 47].

3.3. Effect of Surrounding Medium. The refractive index of the surrounding medium plays a major role in determining the LSPR peak position. If the refractive index of the surrounding medium increases, the LSPR peak gets redshifted as shown in Figure 4.

This can be explained on the basis of resonant condition given in the Mie theory, that is, $\varepsilon_1 = -2\varepsilon_s$, because the real dielectric constant of the noble metal nanoparticle decreases with increasing wavelength and the plasmon resonant wavelength shows redshift with increase in surrounding medium refractive index [2]. Moreover, the surrounding medium becomes denser with increase in its refractive index that leads to the lowering of the restoring force and hence redshift of the LSPR in wavelength region has been found.

3.4. Interaction between the Particles. In practical applications, the effect of interaction between the particles cannot be ignored. In such situations, the interactions between the particles affect the optical properties of metal nanoparticles. When density of the particles embedded in a host material is not very high, then the influence of the neighboring NPs can be included by modifying the host materials dielectric constant as given by effective medium theory with resonance condition [15, 66] given as $\varepsilon_1 = -((2 + f)/(1 - f))\varepsilon_s$, where f represents the filling factor. It may be noted that if the particles size is small as compared to the incident wavelength such that only dipolar mode can be excited in the individual nanoparticle, the LSPR peak shifts to a longer wavelength region as the filling factor increases. This shift is due to the presence of dipole-dipole interaction between the Frohlich modes of the individual particles [66].

3.5. Shape Effect. The LSPR properties of metal nanoparticles can also be tuned by changing the shape or morphology as shown in Figure 5.

For a sufficiently small metal nanoparticle, the resonance wavelength can be obtained by using the relation $\varepsilon' = -((1 - L_\gamma)/L_\gamma)\varepsilon_s$, where ε' is the real dielectric constant of the metal nanoparticle, ε_h represents the dielectric constant of the surrounding medium, and L_γ is called depolarization factor depending on the geometrical parameters of the nanoparticle [14].

Different shape nanoparticles have different geometrical parameters; for example, for spherical nanoparticle there is one geometrical factor which is given by $L = 1/3$ and corresponds to the single LSPR. The resonance wavelength depends on the orientation of incident EF for nonspherical particles. Therefore, for a nanospheroid (prolate or oblate) shape metallic NP, the LSPR splits into the two peaks corresponding to the oscillation of the free electron along (longitudinal mode) and perpendicular (transverse mode) to the long axis. This is due to the two geometrical factors corresponding to its two axes which lead to the generation of two LSPR peaks. The longitudinal mode is much sensitive to

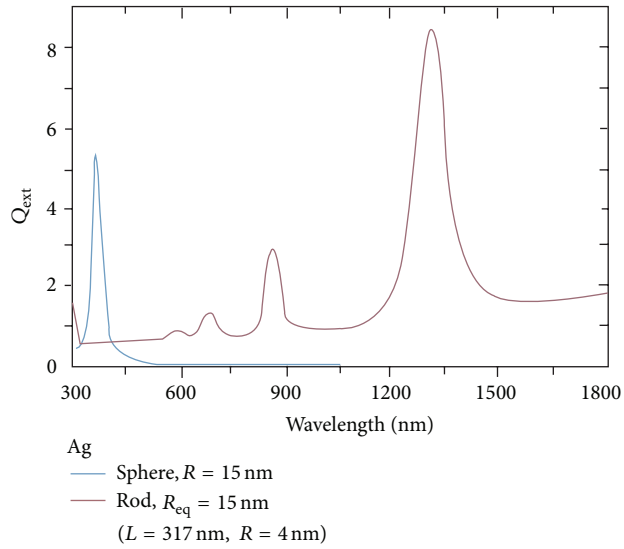

Figure 5: Extinction spectra of the Ag sphere and nanorod of equivalent volume. Reprinted from Coronado et al. [68].

the aspect ratio of the NP. In case of ellipsoid, there are three plasmon resonances corresponding to the oscillation of free electrons along its three axes [2]. This is due to the presence of three geometrical factors along its axes. Further, a general relationship between the surface plasmon resonances and the morphology of each nanoparticle is established in terms of its faces and vertices. As the truncation of nanoparticle increases, the main resonance is blueshifted and overlapping the secondary resonances takes place and, therefore, leads to the increase in the line width of the main resonance. It is also found that nanoparticles with fewer faces and sharper vertices show resonances in a wider range of wavelengths. Moreover, as the nanoparticle becomes more symmetric, the main resonance is always blueshifted [29, 69].

3.6. Substrate Effect. The study of the substrate effect on the optical properties of metallic nanoparticle is very important for practical applications because nanoparticles are mostly synthesized on some kind of substrates. At very large distance from the substrate, there is no interaction of nanoparticle with the substrate and optical properties of nanoparticle are not affected but if the distance between the nanoparticle and substrate is reduced, the substrate induced field on the nanoparticle is no longer homogeneous and leads to the excitation of multipolar modes in addition to the shift of the dipolar one towards the longer wavelength and spectra become wider [14].

4. Theory and Simulations

Several analytical methods such as Mie theory, Gans theory, separation of variables method (SVM), T-matrix, and numerical methods such as finite difference time domain method (FDTD), finite element method (FEM), and discrete dipole approximation (DDA) are available to study the optical properties of nanostructures. Reviews on all these methods have been given by Wriedt [70]. Analytically, it is not possible to study the optical properties of arbitrary shaped metallic nanoparticles such as nanostar and nanocubes. Therefore, in order to overcome this limitation, numerical methods have been developed like discrete dipole approximation (DDA) method and the finite difference time domain (FDTD) method to study the optical properties of arbitrary shaped nanoparticles.

4.1. Discrete Dipole Approximation (DDA). The DDA was first proposed by Purcell & Pennypacker in 1973. The theory of this method was reviewed and developed further by Draine and collaborators [71–73] and recently extended to periodic structures by [74]. This method calculates the scattering and absorption of electromagnetic waves by targets with arbitrary geometries. In this approximation, the whole target is divided into array of N polarizable dipoles, located on a cubic lattice with lattice spacing d, and each cube is characterized by its own polarizability. The dipoles in each cube interact with each other and the incident field, giving rise to a system of linear equations, which are solved by using the fast Fourier transform to obtain the polarizability of each cube. Recent version of DDASCAT7.2, a computer code, efficiently supports fast calculations of the electric field within and near the target using FFT method [75]. The size of the target is given by its effective radius $a_{\text{eff}} = (3V/4\pi)^{1/3}$ with V being the volume of the target. Effective radius is the radius of an equal volume sphere and size parameter of the target is given by $x = ka_{\text{eff}} = 2\pi a_{\text{eff}}/\lambda$ and DDA method is not suitable for larger size parameter and high refractive index. It is also found that $N \geq 10^4$ dipoles are good number for any arbitrary target [29]. The DDA has the drawback that there is a tradeoff between computational time and accuracy.

4.2. Finite Difference Time Domain Method (FDTD). Yee proposed a numerical method called FDTD in 1966, which is a powerful tool for solving Maxwell's equations [76]. The FDTD method is used to compute electromagnetic scattering by nonspherical or inhomogeneous particles. Since surface plasmons are strongly localized at a metal-dielectric interface, accuracy of this method strongly depends on how material boundaries are modeled [70]. The computer code of this method is given in https://www.lumerical.com. In this method, both space and time are divided into discrete segments. Space is segmented into box-shaped "cells" with the electric fields located on the edges of box and the magnetic fields positioned on the faces. Every electric field component (E) is surrounded by four magnetic field components (H) and vice versa. This orientation of the fields is known as the "Yee cell," which is the basis for FDTD simulation. Time is quantized into small steps where each step represents the time required for the field to travel from one cell to the next. The FDTD method involves the discretization of Maxwell's equations in both the time and the space domain in order to find the E and H fields at different positions and at different time steps [77].

From the available literature, it has been found that several experimental studies are present to study the optical

properties of metal-semiconductor nanoparticles but theoretical study of these metal-semiconductor nanoparticles also must be explored to optimize them for various applications. The theoretical study of LSPR based optical properties of multimetallic nanoparticles is also not much explored for plasmon sensing, solar cells, and biomedical applications. It has been found by reviewing the literature that the following work must be explored.

5. Objectives

The objective is to study the LSPR based optical properties such as light scattering efficiency, absorption efficiency, and extinction efficiency of different selected materials of different sizes and shapes to optimize them for applications like solar cells, plasmon sensors, and biomedical applications. The effect of surrounding medium and retardation effects such as surface scattering, depolarization effect, and radiation damping have also to be included for different nanostructures to study

(i) LSPR properties of multimetallic and semiconductor-metal coated nanostructures,

(ii) LSPR properties of clusters such as arrays, layers, and aggregates of multimetallic coated nanostructures,

(iii) LSPR properties of multimetallic alloys,

(iv) LSPR properties of clusters such as arrays, layers, and aggregates of multimetallic alloys,

(v) the optimization of studied materials, size, surrounding medium, and substrate.

5.1. Effect of Surrounding Medium on Light Absorption Characteristics of CdSe, CdS, and CdTe Nanospheres and Their Comparison [78]. The absorption efficiency of cadmium compounds, prospective nanosolar cell materials, as spherical nanoparticles of radius less than 100 nm and effect of surrounding medium refractive index on them have been studied by MiePlot. It is found that the absorption efficiency of CdSe, CdS, and CdTe increases with radius of the nanoparticle and also the UV-visible absorption spectra shift towards red. The maximum of absorption efficiency is observed at 80 nm radius and is in visible region for all the selected materials. Also, with increase in surrounding refractive index, the absorption efficiency is found to be decreasing and absorption spectra are blueshifted. For all these presently selected cadmium compounds, CdTe possesses the highest efficiency as compared to both CdS and CdSe.

5.2. Scattering Efficiency and LSPR Tunability of Bimetallic Ag, Au, and Cu Nanoparticles [79]. Scattering efficiencies of Ag-Cu, Ag-Au, and Au-Cu alloy nanoparticles are studied based on Mie theory for their possible applications in solar cells. The effect of size (radius), surrounding medium, and alloy composition on the scattering efficiency at the localized surface plasmon resonance (LSPR) wavelengths has been reported. In the alloy nanoparticles of $Ag_{1-x}Cu_x$, $Au_{1-x}Cu_x$, and $Ag_{1-x}Au_x$, the scattering efficiency gets redshifted with increase in x. Moreover, the scattering efficiency enhancement can be tuned and controlled with both the alloy composition and the surrounding medium refractive index. A linear relationship which is in good agreement with the experimental observations between the scattering efficiency and metal composition in the alloys is found. The effect of nanoparticle size and LSPR wavelength (scattering peak position) on the full width half maxima and scattering efficiency has also been studied. Comparison of Au-Ag, Au-Cu, and Ag-Cu alloy nanoparticles with 50 nm radii shows the optical response of Ag-Cu alloy nanoparticle with wide bandwidth in the visible region of the electromagnetic spectrum making them suitable for plasmonic solar cells. Further, the comparison of Ag-Cu alloy and core-shell nanoparticles of similar size and surrounding medium shows that Cu-Ag nanoparticle exhibits high scattering efficiency with nearly the same bandwidth.

5.3. Tailoring LSPR Based Absorption and Scattering Efficiencies of Semiconductor Coated Au Nanoshells [80]. Absorption and scattering efficiencies of semiconductor coated Au nanoshell have been studied by extended Mie theory for their possible applications in solar cells, optical imaging, photothermal applications, and so forth. The effect of Au shell layer thickness, core size, and surrounding medium on the absorption and scattering efficiencies at the localized surface plasmon resonance (LSPR) wavelengths has been reported. It has been found that both the absorption and scattering LSPR peak position get blueshifted, that is, infrared (IR) to visible, with increase in Au shell layer thickness from 2 nm to 10 nm, whereas shifts towards red with increase in surrounding refractive index. It has also been found that the spectra are redshifted with increase in the core radius from 20 nm to 40 nm, while keeping the shell thickness the same. The effect of shell thickness on the absorption peak position and absorption line width has also been studied. Hence, the optical response of both CdSe and CdTe coated Au nanoshells can be tuned and controlled from IR to visible region of the electromagnetic (EM) spectrum. Finally, the CdSe coated Au nanoshell exhibits high scattering and absorption efficiencies in comparison to CdTe coated nanoshell.

The CdSe/CdTe semiconductor nanoparticles are also used for biomedical applications as explained by [81]; therefore, to increase their potential and biocompatibility, these semiconductors are considered to be coated with Au so that their toxicity can be reduced because of a better biocompatibility of Au. Further, their efficiency can also be increased in the NIR region for better biomedical applications. Thus, there is a large tunability from visible to infrared region in this case as compared to CdTe/CdSe and almost in the same region as for Au nanorods [82] and nanoshells [83].

6. Conclusion

Selection of materials with suitable combinations (pure, alloys, and coated) and their physical parameters like size and shape along with their surroundings play a great role in the tunability of LSPR based optical properties for their possible use in a specific application like plasmonic sensors

and biomedical applications and to enhance the efficiency of thin-film solar cells. This communication briefly highlighted the latest developments in this direction so that selection of materials can pave the way of their utilization in any application with desired outcomes. The effect of nanoparticle size, shape, surrounding medium, interaction between the particles, and composition in alloys on the LSPR has been studied. The retardation effects such as radiation damping, dynamic depolarization, and surface scattering have also been included. Several analytical and numerical methods are reviewed for the study of optical properties.

(i) Bimetallic systems give more freedom in selection of metal composition with better stability and tunability for various plasmonic applications.

(ii) The absorption of semiconductor materials can be enhanced by combining the semiconductor with noble metal nanoparticles of suitable choice.

Conflict of Interests

The authors declare that there is no conflict of interests regarding the publication of this paper.

Acknowledgment

The first author, Amit Bansal, would like to thank SLIET authorities.

References

[1] B. E. Hutter and J. H. Fendler, "Exploitation of localized surface plasmon resonance," *Advanced Materials*, vol. 16, no. 19, pp. 1685–1706, 2004.

[2] K. L. Kelly, E. Coronado, L. L. Zhao, and G. C. Schatz, "The optical properties of metal nanoparticles: the influence of size, shape, and dielectric environment," *Journal of Physical Chemistry B*, vol. 107, no. 3, pp. 668–677, 2003.

[3] G. H. Chan, J. Zhao, E. M. Hicks, G. C. Schatz, and R. P. van Duyne, "Plasmonic properties of copper nanoparticles fabricated by nanosphere lithography," *Nano Letters*, vol. 7, no. 7, pp. 1947–1952, 2007.

[4] J. S. Sekhon and S. S. Verma, "Refractive Index Sensitivity Analysis of Ag, Au, and Cu Nanoparticles," *Plasmonics*, vol. 6, no. 2, pp. 311–317, 2011.

[5] M. Alsawafta, M. Wahbeh, and V.-V. Truong, "Plasmonic modes and optical properties of gold and silver ellipsoidal nanoparticles by the discrete dipole approximation," *Journal of Nanomaterials*, vol. 2012, Article ID 457968, 10 pages, 2012.

[6] J. Grand, P.-M. Adam, A.-S. Grimault et al., "Optical extinction spectroscopy of oblate, prolate and ellipsoid shaped gold nanoparticles: experiments and theory," *Plasmonics*, vol. 1, no. 2–4, pp. 135–140, 2006.

[7] J. Sung, K. M. Kosuda, J. Zhao, J. W. Elam, K. G. Spears, and R. P. van Duyne, "Stability of silver nanoparticles fabricated by nanosphere lithography and atomic layer deposition to femtosecond laser excitation," *Journal of Physical Chemistry C*, vol. 112, no. 15, pp. 5707–5714, 2008.

[8] J. Conde, G. Doria, and P. Baptista, "Noble metal nanoparticles applications in cancer," *Journal of Drug Delivery*, vol. 2012, Article ID 751075, 12 pages, 2012.

[9] M. K. Hossain, Y. Kitahama, G. G. Huang, X. Han, and Y. Ozaki, "Surface-enhanced raman scattering: realization of localized surface plasmon resonance using unique substrates and methods," *Analytical and Bioanalytical Chemistry*, vol. 394, no. 7, pp. 1747–1760, 2009.

[10] J. S. Sekhon and S. S. Verma, "Rational selection of nanorod plasmons: material, size, and shape dependence mechanism for optical sensors," *Plasmonics*, vol. 7, no. 3, pp. 453–459, 2012.

[11] G. Doria, J. Conde, B. Veigas et al., "Noble metal nanoparticles for biosensing applications," *Sensors*, vol. 12, no. 2, pp. 1657–1687, 2012.

[12] K. R. Catchpole and A. Polman, "Plasmonic solar cells," *Optics Express*, vol. 16, no. 26, pp. 21793–21800, 2008.

[13] S. Pillai and M. A. Green, "Plasmonics for photovoltaic applications," *Solar Energy Materials and Solar Cells*, vol. 94, no. 9, pp. 1481–1486, 2010.

[14] C. Noguez, "Surface plasmons on metal nanoparticles: the influence of shape and physical environment," *Journal of Physical Chemistry C*, vol. 111, no. 10, pp. 3606–3619, 2007.

[15] A. Moores and F. Goettmann, "The plasmon band in noble metal nanoparticles: an introduction to theory and applications," *New Journal of Chemistry*, vol. 30, no. 8, pp. 1121–1132, 2006.

[16] K.-S. Lee and M. A. El-Sayed, "Gold and silver nanoparticles in sensing and imaging: sensitivity of plasmon response to size, shape, and metal composition," *Journal of Physical Chemistry B*, vol. 110, no. 39, pp. 19220–19225, 2006.

[17] N. E. Motl, E. Ewusi-Annan, I. T. Sines, L. Jensen, and R. E. Schaak, "Au-Cu alloy nanoparticles with tunable compositions and plasmonic properties: experimental determination of composition and correlation with theory," *Journal of Physical Chemistry C*, vol. 114, no. 45, pp. 19263–19269, 2010.

[18] M. G. Blaber, M. D. Arnold, and M. J. Ford, "A review of the optical properties of alloys and intermetallics for plasmonics," *Journal of Physics Condensed Matter*, vol. 22, no. 14, Article ID 143201, 2010.

[19] G. Mie, "Beiträge zur Optik trüber Medien, speziell kolloidaler Metallösungen," *Annalen der Physik*, vol. 330, no. 3, pp. 377–445, 1908.

[20] S. Link, M. B. Mohamed, and M. A. El-Sayed, "Simulation of the optical absorption spectra of gold nanorods as a function of their aspect ratio and the effect of the medium dielectric constant," *Journal of Physical Chemistry B*, vol. 103, no. 16, pp. 3073–3077, 1999.

[21] A. L. Aden and M. Kerker, "Scattering of electromagnetic waves from two concentric spheres," *Journal of Applied Physics*, vol. 22, no. 10, pp. 1242–1246, 1951.

[22] D. W. Mackowski, R. A. Altenkirch, and M. P. Menguc, "Internal absorption cross sections in a stratified sphere," *Applied Optics*, vol. 29, no. 10, pp. 1551–1559, 1990.

[23] B. R. Johnson, "Light scattering by a multilayer sphere," *Applied Optics*, vol. 35, no. 18, pp. 3286–3296, 1996.

[24] E. E. M. Khaled and M. F. Salem, "Scattering of an electromagnetic beam by a radially inhomogeneous sphere," in *Proceedings of the 17th National Radio Science Conference (NRCS '00)*, 2000.

[25] W. Yang, "Improved recursive algorithm for light scattering by a multilayered sphere," *Applied Optics*, vol. 42, no. 9, pp. 1710–1720, 2003.

[26] C. F. Bohren and D. R. Huffman, *Absorption and Scattering of Light by Small Particles*, Wiley, New York, NY, USA, 1998.

[27] O. P. Rodriguez, P. P. G. Perez, and U. Pal, "MieLab: a software tool to perform calculations on the scattering of electromagnetic waves by multilayered spheres," *International Journal of Spectroscopy*, vol. 2011, Article ID 583743, 10 pages, 2011.

[28] C. Langhammer, Z. Yuan, I. Zorić, and B. Kasemo, "Plasmonic properties of supported Pt and Pd nanostructures," *Nano Letters*, vol. 6, no. 4, pp. 833–838, 2006.

[29] I. O. Sosa, C. Noguez, and R. G. Barrera, "Optical properties of metal nanoparticles with arbitrary shapes," *Journal of Physical Chemistry B*, vol. 107, no. 26, pp. 6269–6275, 2003.

[30] Y. W. Ma, Z. W. Wu, L. H. Zhang, J. Zhang, G. S. Jian, and S. Pan, "Theoretical study of the local surface plasmon resonance properties of silver nanosphere clusters," *Plasmonics*, vol. 8, no. 3, pp. 1351–1360, 2013.

[31] V. G. Stoleru and E. Towe, "Optical properties of nanometer-sized gold spheres and rods embedded in anodic alumina matrices," *Applied Physics Letters*, vol. 85, no. 22, article 3, pp. 5152–5154, 2004.

[32] G. Yin, S.-Y. Wang, M. Xu, and L.-Y. Chen, "Theoretical calculation of the optical properties of gold nanoparticles," *Journal of the Korean Physical Society*, vol. 49, no. 5, pp. 2108–2111, 2006.

[33] A. Sureka and V. Santhanam, "Optical properties of metal nanoparticles using DDA," *Journal of Young Investigators*, vol. 25, no. 4, pp. 66–72, 2013.

[34] F. Hao and P. Nordlander, "Efficient dielectric function for FDTD simulation of the optical properties of silver and gold nanoparticles," *Chemical Physics Letters*, vol. 446, no. 1–3, pp. 115–118, 2007.

[35] O. Peña-Rodríguez and U. Pal, "Effects of surface oxidation on the linear optica properties of Cu nanoparticles," *Journal of the Optical Society of America B: Optical Physics*, vol. 28, no. 11, pp. 2735–2739, 2011.

[36] K. S. Tan and K. Y. Cheong, "Advances of Ag, Cu, and Ag-Cu alloy nanoparticles synthesized via chemical reduction route," *Journal of Nanoparticle Research*, vol. 15, article 1537, 2013.

[37] Y. Nishijima and S. Akiyama, "Unusual optical properties of the Au/Ag alloy at the matching mole fraction," *Optical Materials Express*, vol. 2, no. 9, pp. 1226–1235, 2012.

[38] O. Peña-Rodríguez and U. Pal, "Enhanced plasmonic behavior of bimetallic (Ag-Au) multilayered spheres," *Nanoscale Research Letters*, vol. 6, article 279, 2011.

[39] R. D. Averitt, S. L. Westcott, and N. J. Halas, "Linear optical properties of gold nanoshells," *Journal of the Optical Society of America B: Optical Physics*, vol. 16, no. 10, pp. 1824–1832, 1999.

[40] L. Lu, G. Burkey, I. Halaciuga, and D. V. Goia, "Core-shell gold/silver nanoparticles: synthesis and optical properties," *Journal of Colloid and Interface Science*, vol. 392, pp. 90–95, 2013.

[41] W. Bhagathsingha and A. S. Nesaraj, "Low temperature synthesis and thermal properties of Ag-Cu alloy nanoparticles," *Transactions of Nonferrous Metals Society of China*, vol. 23, no. 1, pp. 128–133, 2013.

[42] H. T. Beyene, V. S. K. Chakravadhanula, C. Hanisch et al., "Vapor phase deposition, structure, and plasmonic properties of polymer-based composites containing Ag-Cu bimetallic nanoparticles," *Plasmonics*, vol. 7, no. 1, pp. 107–114, 2012.

[43] A. Steinbrück, O. Stranik, A. Csaki, and W. Fritzsche, "Sensoric potential of gold-silver core-shell nanoparticles," *Analytical and Bioanalytical Chemistry*, vol. 401, no. 4, pp. 1241–1249, 2011.

[44] A. Shah, L.-U. Latif-Ur-Rahman, R. Qureshi, and Z.-U. Zia-Ur-Rehman, "Synthesis, characterization and applications of bimetallic (Au-Ag, Au-Pt, Au-Ru) alloy nanoparticles," *Reviews on Advanced Materials Science*, vol. 30, no. 2, pp. 133–149, 2012.

[45] M. Taner, N. Sayar, I. G. Yulug, and S. Suzer, "Synthesis, characterization and antibacterial investigation of silver-copper nanoalloys," *Journal of Materials Chemistry*, vol. 21, no. 35, pp. 13150–13154, 2011.

[46] M. Valodkar, S. Modi, A. Pal, and S. Thakore, "Synthesis and anti-bacterial activity of Cu, Ag and Cu-Ag alloy nanoparticles: a green approach," *Materials Research Bulletin*, vol. 46, no. 3, pp. 384–389, 2011.

[47] L. U. Rahman, R. Qureshi, M. M. Yasinzai, and A. Shah, "Synthesis and spectroscopic characterization of Ag-Cu alloy nanoparticles prepared in various ratios," *Comptes Rendus Chimie*, vol. 15, no. 6, pp. 533–538, 2012.

[48] Z. Kiani, Y. Abdi, and E. Arzi, "Low temperature formation of silver and silver-copper alloy nano-particles using plasma enhanced hydrogenation and their optical properties," *World Journal of Nano Science and Engineering*, vol. 2, pp. 142–147, 2012.

[49] S. Liu, G. Chen, P. N. Prasad, and M. T. Swihart, "Synthesis of monodisperse Au, Ag, and Au-Ag alloy nanoparticles with tunable size and surface plasmon resonance frequency," *Chemistry of Materials*, vol. 23, no. 18, pp. 4098–4101, 2011.

[50] T. Som and B. Karmakar, "Core-shell Au-Ag nanoparticles in dielectric nanocomposites with plasmon-enhanced fluorescence: a new paradigm in antimony glasses," *Nano Research*, vol. 2, no. 8, pp. 607–616, 2009.

[51] Y.-W. Ma, J. Zhang, L.-H. Zhang, G.-S. Jian, and S.-F. Wu, "Theoretical analysis the optical properties of multi-coupled silver nanoshell particles," *Plasmonics*, vol. 6, no. 4, pp. 705–713, 2011.

[52] D. L. Ferreira, F. O. Silva, L. C. D. S. Viol, P. Licínio, M. A. Schiavon, and J. L. A. Alves, "Theoretical and experimental studies of stressed nanoparticles of II-VI semiconductors," *Journal of Chemical Physics*, vol. 132, no. 1, Article ID 014107, 2010.

[53] M. I. B. Utama, J. Zhang, R. Chen et al., "Synthesis and optical properties of II-VI 1D nanostructures," *Nanoscale*, vol. 4, pp. 1422–1435, 2012.

[54] M. M. Chili, V. S. R. R. R. Pullabhotla, and N. Revaprasadu, "Synthesis of PVP capped gold nanoparticles by the UV-irradiation technique," *Materials Letters*, vol. 65, no. 17-18, pp. 2844–2847, 2011.

[55] M. Li, X.-F. Yu, S. Liang et al., "Synthesis of Au-CdS core-shell hetero-nanorods with efficient exciton-plasmon interactions," *Advanced Functional Materials*, vol. 21, no. 10, pp. 1788–1794, 2011.

[56] A. K. Pradhan, R. B. Konda, H. Mustafa et al., "Surface plasmon resonance in CdSe semiconductor coated with gold nanoparticles," *Optics Express*, vol. 16, no. 9, pp. 6202–6208, 2008.

[57] R. Bardhan, N. K. Grady, T. Ali, and N. J. Halas, "Metallic nanoshells with semiconductor cores: optical characteristics modified by core medium properties," *ACS Nano*, vol. 4, no. 10, pp. 6169–6179, 2010.

[58] L. Zhou, X. Yu, and J. Zhu, "Metal-core/semiconductor-shell nanocones for broadband solar absorption enhancement," *Nano Letters*, vol. 14, no. 2, pp. 1093–1098, 2014.

[59] D. M. Schaadt, B. Feng, and E. T. Yu, "Enhanced semiconductor optical absorption via surface plasmon excitation in metal

nanoparticles," *Applied Physics Letters*, vol. 86, no. 6, Article ID 063106, pp. 1–3, 2005.

[60] T. Repan and S. Pikker, "Increased efficiency inside the CdTe solar cell absorber caused by plasmonic metal nanoparticles," *Energy Procedia*, vol. 44, pp. 229–233, 2014.

[61] E. Shaviv, O. Schubert, M. Alves-Santos et al., "Absorption properties of metal-semiconductor hybrid nanoparticles," *ACS Nano*, vol. 5, no. 6, pp. 4712–4719, 2011.

[62] M. Achermann, "Exciton-plasmon interactions in metal-semiconductor nanostructures," *Journal of Physical Chemistry Letters*, vol. 1, no. 19, pp. 2837–2843, 2010.

[63] K. Easawi, M. Nabil, T. Abdallah, S. Negm, and H. Talaat, "Plasmonic absorption enhancement in Au/CdS nanocomposite," *Proceedings of World Academy of Science, Engineering and Technology*, vol. 61, pp. 548–551, 2012.

[64] J. S. Sekhon and S. S. Verma, "Optimal dimensions of gold nanorod for plasmonic nanosensors," *Plasmonics*, vol. 6, no. 1, pp. 163–169, 2011.

[65] S. Link and M. A. El-Sayed, "Size and temperature dependence of the plasmon absorption of colloidal gold nanoparticles," *Journal of Physical Chemistry B*, vol. 103, no. 21, pp. 4212–4217, 1999.

[66] S. Hayashi and T. Okamoto, "Plasmonics: visit the past to know the future," *Journal of Physics D: Applied Physics*, vol. 45, no. 43, Article ID 433001, 2012.

[67] E. Hutter, J. H. Fendler, and D. Roy, "Surface plasmon resonance studies of gold and silver nanoparticles linked to gold and silver substrates by 2-aminoethanethiol and 1,6-hexanedithiol," *Journal of Physical Chemistry B*, vol. 105, no. 45, pp. 11159–11168, 2001.

[68] E. A. Coronado, E. R. Encina, and F. D. Stefani, "Optical properties of metallic nanoparticles: manipulating light, heat and forces at the nanoscale," *Nanoscale*, vol. 3, no. 10, pp. 4042–4059, 2011.

[69] E. Stefan Kooij and B. Poelsema, "Shape and size effects in the optical properties of metallic nanorods," *Physical Chemistry Chemical Physics*, vol. 8, no. 28, pp. 3349–3357, 2006.

[70] T. Wriedt, "Light scattering theories and computer codes," *Journal of Quantitative Spectroscopy and Radiative Transfer*, vol. 110, no. 11, pp. 833–843, 2009.

[71] B. T. Draine, "The discrete-dipole approximation and its application to interstellar graphite grains," *Journal of Astrophysics*, vol. 333, pp. 848–872, 1988.

[72] B. T. Draine and J. Goodman, "Beyond Clausius-Mossotti: wave propagation on a polarizable point lattice and the discrete dipole approximation," *Astrophysical Journal Letters*, vol. 405, no. 2, pp. 685–697, 1993.

[73] B. T. Draine and P. J. Flatau, "Discrete-dipole approximation for scattering calculations," *Journal of the Optical Society of America A: Optics and Image Science, and Vision*, vol. 11, no. 4, pp. 1491–1499, 1994.

[74] B. T. Draine and P. J. Flatau, "Diserete-dipole approximation for periodic targets: theory and tests," *Journal of the Optical Society of America A: Optics and Image Science, and Vision*, vol. 25, no. 11, pp. 2693–2703, 2008.

[75] P. J. Flatau and B. T. Draine, "Fast near field calculations in the discrete dipole approximation for regular rectilinear grids," *Optics Express*, vol. 20, no. 2, pp. 1247–1252, 2012.

[76] K. Yee, "Numerical solution of initial boundary value problems involving Maxwell's equations in isotropic media," *IEEE Transactions on Antennas and Propagation*, vol. 14, no. 3, pp. 302–307, 1966.

[77] Z. L. Yang, Q. H. Li, F. X. Ruan et al., "FDTD for plasmonics: applications in enhanced Raman spectroscopy," *Chinese Science Bulletin*, vol. 55, no. 24, pp. 2635–2642, 2010.

[78] A. Bansal, J. S. Sekhon, and S. S. Verma, "Effect of surrounding medium on light absorption characteristics of CdSe, CdS & CdTe nanospheres and their comparison," *AIP Conference Proceedings*, vol. 1536, pp. 267–268, 2013.

[79] A. Bansal, J. S. Sekhon, and S. S. Verma, "Scattering efficiency and LSPR tunability of bimetallic Ag, Au, and Cu nanoparticles," *Plasmonics*, vol. 9, no. 1, pp. 143–150, 2014.

[80] A. Bansal and S. S. Verma, "Tailoring LSPR-based absorption and scattering efficiencies of semiconductor-coated Au nanoshells," vol. 9, no. 2, pp. 335–341, 2014.

[81] Y. Wang, "Luminescent CdTe and CdSe semiconductor nanocrystals: preparation, optical properties and applications," *Journal of Nanoscience and Nanotechnology*, vol. 8, no. 3, pp. 1068–1091, 2008.

[82] W. Ni, X. Kou, Z. Yang, and J. Wang, "Tailoring longitudinal surface plasmon wavelengths, scattering and absorption cross sections of gold nanorods," *ACS Nano*, vol. 2, no. 4, pp. 677–686, 2008.

[83] S. J. Oldenburg, J. B. Jackson, S. L. Westcott, and N. J. Halas, "Infrared extinction properties of gold nanoshells," *Applied Physics Letters*, vol. 75, no. 19, pp. 2897–2899, 1999.